$k_{inside}$ = rate constant per unit volume of reactor for reaction occurring inside catalyst [$sec^{-1}$]
$L_p$ = height of cylindrical catalyst [cm]
$L_R$ = reactor length [cm]
$m$ = Thiele modulus ($=R\sqrt{k/D_e}$) [—]
$p$ = pressure [atm]
$PeB$ = $u_{in}L_p/D_e$ [—]
$R$ = radius of spherical (cylindrical) catalyst [cm]
$r$ = radial co-ordinate [cm]
$Re_p$ = Reynolds number ($=D_p\rho u/\mu$) [—]
$Re_m$ = Reynolds number ($=\phi D_p\rho u/6(1-\varepsilon_{out})$) [—]
$Sc$ = Schmidt number ($=\nu/D$) [—]
$Sh$ = Sherwood number ($=k_{film}D_p/D$) (Eq. (12)) [—]
$T$ = average contact time based on superficial flow rate [sec]
$u_{out}$, and $u$ = superficial velocity in catalyst bed [cm/sec]
$u_{in}$ = superficial velocity of intraparticle flow [cm/sec]
$X$ = conversion of reactant [—]
$z$ = longitudinal co-ordinate [cm]
$\varepsilon$ = void fraction [—]
$\mu$ = viscosity [g/cm·sec]
$\rho$ = density [$g/cm^3$]
$\tau$ = residence time [sec]
$\phi$ = shape factor [—]
$\omega$ = ratio of radius to height in cylindrical pellet [—]

〈Subscripts〉
in = refers to values characterizing fine particles which aggregate to form a pellet
out = refers to values characterizing catalyst bed

**Literature Cited**


1) Aris, R.: *Chem. Eng.Sci.*, **6**, 262 (1957)
2) Carman, P. C.: *Trans. Inst. Chem. Engrs. (London)*, **15**, 150 (1937)
3) Wakao, N., T. Oshima, and S. Yagi: *Kagaku Kōgaku*, **22**, 780 (1958)
4) Komiyama, H.: Dissertation, Univ. of Tokyo (1972)


# SIMULATION OF PYROLYSIS OF PARAFFINIC HYDROCARBON BINARY MIXTURES*


MITSUO MURATA, NORIO TAKEDA AND SHOZABURO SAITO
*Department of Chemical Engineering, Tohoku University, Sendai*



**Pyrolysis of several binary mixtures composed of ethane, propane, *n*-butane, *i*-butane, and neopentane at small extents of reaction has been studied in order to extend the method previously proposed for a single component to the prediction of the initial pyrolytic products from mixtures. In the pyrolysis of each binary system, generally, one component disappears faster than when it is pyrolyzed by itself, while the rate of disappearance of the other component changes little. In particular, the rate of propane decomposition increases by a maximum of 2.8 times in the propane-neopentane mixture.**

**The product distributions from mixtures are approximately uniform with the extents of reaction, being analogous to the case of single components. The distributions of the mixtures predicted on the basis of the results for the single components are found to be in good agreement with those experimentally observed, with the assumption that the selectivity to products of a single component is maintained in its mixture system. The reaction can be accounted for by a free-radical chain mechanism, and it is confirmed that the change of overall reaction rate, affected by the existence of the other component, depends on the concentration of hydrogen atoms and methyl radicals, and that the initiation reaction rate of each component has a central role.**


## Introduction

The pyrolysis of individual paraffinic hydrocarbons has already been studied comprehensively, and the knowledge accumulated thereby has enabled us to predict initial product distributions by using a computer[9,18,26]. It has not, however, been clarified whether or not the above predicting methods for a single component can be applied directly to mixtures. The pyrolysis of hydrocarbon mixtures is of great significance not only from an engineering design standpoint but also from the standpoint of elucidation of the reaction mechanism, since it gives us new information which cannot be gained from the pyrolysis of single components.

Recent studies on the pyrolysis of paraffinic hydrocarbon mixtures have been carried out by Zdonic *et al.*[30,31], Tanji[27], and Kubota *et al.*[13] Zdonic *et al.* examined the initial products of the ethane-propane mixture based on a free-radical chain mechanism and


* Received on September 1, 1973
Presented at the 6th Autumn Meeting of The Soc. of Chem. Engrs., Japan, Tokyo, 1972 (Preprint, p. 223)


〒980 仙台市荒巻字青葉
東北大学工学部化学工学科 斎藤正三郎

indicated that the product distribution from either of the two feed constituents is not influenced by the presence of the other component and that it is the same as that from each single component. They also concluded that when a binary mixture was pyrolyzed, the radicals generated by the pyrolysis of the less refractory compound accelerate the decomposition of the more refractory constituent. Tanji found that addition of 5 mole% of *n*-hexadecane to cyclopentane, methyl-cyclohexane, and *n*-heptane, respectively, increased the overall rate of pyrolysis in each case. Kubota *et al.* reported that there was no measurable change in the initial decomposition rate of propane added with 10 to 40 mole % of ethane.

The pyrolysis of paraffinic hydrocarbons mixed with olefinic compounds has also been studied for the elucidation of the high-conversion pyrolysis mechanism of individual paraffinic hydrocarbons[8,10,12,13,24,29]. These studies generally showed that the decomposition reactions of paraffinic hydrocarbons were inhibited, while those of olefinic constituents were accelerated. Robinson *et al.*[24] inferred that the great increase in the decomposition rate of propylene, in the propane-propylene mixture, was due to the action of chain carriers generated by propane pyrolysis.

As stated above, it is generally found that the components will interact with each other through the action of radicals produced from each component in the pyrolysis of paraffinic hydrocarbon mixtures. However, the mechanism of the interaction has not yet been elucidated, and the quantitative estimation of the change of decomposition rate for each component is very difficult.

The purpose of this work was to clarify the influence on reaction rate and product distribution of the presence of the other component in binary paraffinic hydrocarbon mixtures composed of ethane, propane, *n*-butane, *i*-butane, and neopentane by a free-radical chain mechanism. Many previous investigations of the pyrolysis of the above hydrocarbons have provided different values of the initial rate. Therefore, to compare the reaction rates of individual components with those of mixtures, each individual component was pyrolyzed before the binary mixture.

## 1. Experimental Apparatus and Procedure

The experiments were performed with two kinds of apparatus under atmospheric pressure in order to make clear the influence of different experimental procedures on the observations. One apparatus was of the conventional flow type and the other was a modified flow apparatus which had been adapted

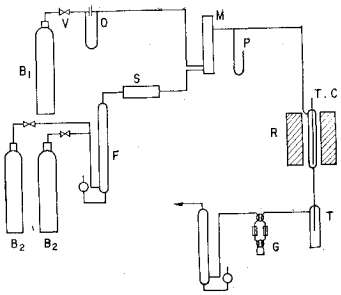


$B_1$: nitrogen bomb
$B_2$: feed bomb
V: needle valve
O: orifice flowmeter
F: soap-film flowmeter
S: silica gel tube
M: mixer
P: manometer
T.C: thermocouple
R: reactor
T: trap
G: gas sampling cell

**Fig. 1 Schematic diagram of experimental apparatus**

to maintain better isothermal conditions (hereafter termed the isothermal apparatus). The details of the isothermal apparatus were described in a previous paper[19]. Unless otherwise mentioned, the conventional flow apparatus was used, and its schematic diagram is shown in **Fig. 1**. The reactant gases and nitrogen diluent, metered separately, were flow-controlled by adjustment of needle valves; they were mixed in a tube packed with glass spheres and charged in the reactor. The gas leaving the reactor was quickly cooled in an ice-trap, and the volume of the uncondensed gas was measured before its release to the air. The reactor used was constructed of straight, 20 cm pieces of quartz tubing (19 mm internal diameter) and had a quartz thermocouple well (4 mm external diameter). Quartz chips of 4 to 8 mm in length were packed in the reactor. The reactor volume per unit length was 1.14 ml/cm. The reactor was maintained inside a bronze block electrically heated at a temperature controlled to within $\pm 0.5$°C. During each experiment, temperatures were measured at about 1 cm intervals along the reactor, using a chromel-alumel thermocouple. Each point was assigned a weight proportional to the rate of reaction at that temperature, and the effective lengths of the reaction zones were calculated*. The average residence time, $t$, of the gas in the reaction zone was defined as

$$t = V_{av} \Big/ F \cdot \left(\frac{760}{P}\right)\left(\frac{T_{av}}{273}\right) \qquad (1)$$

where the flow rate, $F$, was the average value of inlet and outlet of the reactor since the expansion of the gas was small under the present conditions.

Prepurified-grade nitrogen (99.999% minimum purity) was used as the diluent; the oxygen content had to be kept low since it caused a large change in the initial rate of hydrocarbon pyrolysis. The hydrocarbons used were instrument-grade (99.5% minimum purity).

Samples of the reactor effluent stream were analyzed with a gas chromatograph equipped with a thermal conductivity detector. Two columns were used here. One is a 3 m molecular sieve 13X column, and the other a 4 m 1.5% squarane and 38% DMF on $\gamma$-

* Activation energies used here were as follows: $C_3H_8$: 60, $n$-$C_4H_{10}$: 55, $i$-$C_4H_{10}$: 55 and neo-$C_5H_{12}$: 50 [kcal/mole] These values were also used in mixture system[27].

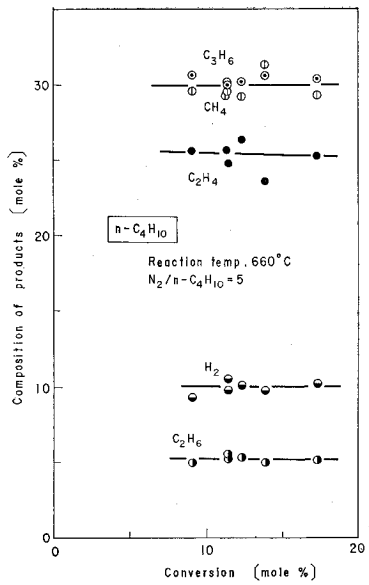


**Fig. 2 Initial product distribution from *n*-butane pyrolysis**

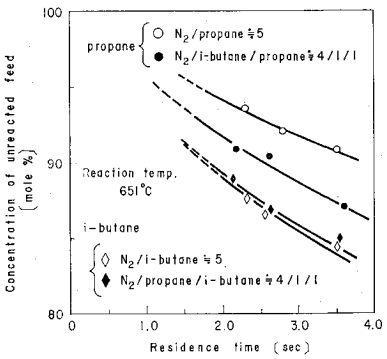


**Fig. 5 Comparison of reaction rates observed using the isothermal apparatus**

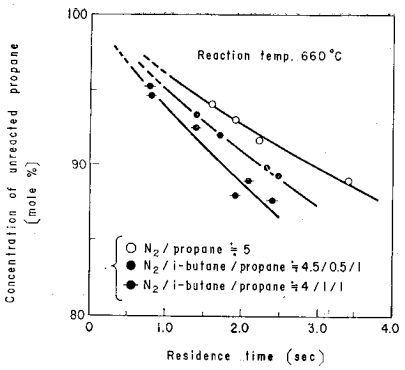


**Fig. 3 Comparison of reaction rates of propane between single component and binary mixture system**

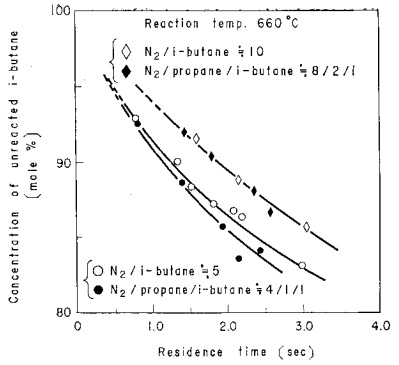


**Fig. 4 Comparison of reaction rates of *i*-butane between single component and binary mixture system**

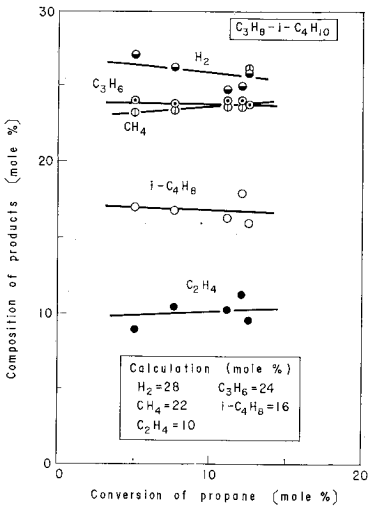


**Fig. 6 Initial product distribution from pyrolysis of propane-*i*-butane mixture (660°C)**

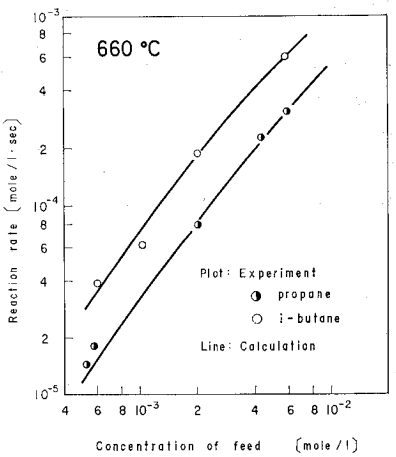


**Fig. 7 Comparison of reaction rates of propane and *i*-butane between experimental and calculated values**

alumina column. The former was operated at 50°C with Ar carrier gas (30 m*l*/min), and the latter at 0°C with He carrier gas (30 m*l*/min).

## 2. Experimental Results and Discussion

### 2. 1 Pyrolysis of individual paraffinic hydrocarbons

Ethane, propane, *n*-butane, *i*-butane, and neopentane were pyrolyzed at temperatures ranging from 650 to 690°C, with residence times from 0.8 to 3.8 sec, and with nitrogen/hydrocarbon mole ratios from 1 to 20. In every case, the distribution of major products seemed to be independent of extent of reaction under the present conditions. An example is shown in **Fig. 2** for *n*-butane pyrolysis.

### 2. 2 Pyrolysis of binary mixtures of paraffinic hydrocarbons

The five binary mixtures ethane-propane, propane-*i*-butane, propane-neopentane, *i*-butane-neopentane, and *n*-butane-*i*-butane were pyrolyzed at temperatures ranging from 650 to 690°C, with residence times from 0.8 to 3.6 sec and mole ratios of two constituents of 0.5 and 1. Typical results of the initial rates of propane and *i*-butane, in the propane-*i*-butane mixture, at 660°C are compared with those of pyrolysis of the corresponding single components, under the same condition of initial concentration, in **Figs. 3** and **4**. Figure 3 shows explicitly that the decomposition of propane is accelerated by addition of *i*-butane from the early stage of the reaction, and that the acceleration increases with increasing *i*-butane concentration. On the other hand, as shown in Fig. 4, the change of decomposition rate of *i*-butane by addition of propane is very small. It is independent of the amount of propane added. The results at 686°C are similar to those described above.

The same system was pyrolyzed by using the isothermal apparatus at 651°C with *i*-butane/propane mole ratio of 1. The relations between the unreacted feed mole ratio and the residence time are given in **Fig. 5** for propane and *i*-butane. These tendencies shown are nearly consistent with those obtained by the conventional flow apparatus shown in Figs. 3 and 4, though a slight inhibiting effect on *i*-butane decomposition is observed. This means that it is

possible by using the conventional flow apparatus to examine whether or not the presence of the other component causes the change in decomposition rate. The individual initial decomposition rates in each binary system are compared with those observed in a single component system in **Table 1**. The initial decomposition rate of each component in single and binary systems was calculated at the same conversion by using the following equation*:

$$R_p = -dC/dt \cong C_o x/t \qquad (2)$$

The value of $R_p$ should, if possible, be determined at $x=0$, but it was done here at $x=0.08$ since the data near $x=0$ could not be obtained precisely. The $R_p$ calculated by using Eq. (2), however, may be enough to discuss the influence of the presence of the other component on the decomposition rate. The tabulated data show that the reaction of one component is clearly accelerated, while that of the other is hardly affected by the coexisting component in each binary mixture except in the case of the ethane-propane mixture. However, the degree of acceleration varies in a complex manner according to the specific mixture. The result given by the ethane-propane mixture, on the other hand, shows that there is no measurable change in the decomposition rates of both components. This agrees well with the result of Kubota *et al.* The product distributions, under the experimental conditions, are nearly independent of the extent of reaction. The result, for example, for the propane-*i*-butane mixture is illustrated in **Fig. 6**. It is in satisfactory agreement with the calculated value also shown in Fig. 6. The calculated value was obtained from the conversion of each component in the binary system, on the assumption that the selectivity to products of a single component was unchanged in a mixture system. The calculation procedure is shown in **Appendix 1**.

### 2. 3 Simulation of the pyrolysis of binary mixtures by free-radical chain reaction schemes

According to the experimental results of the individual compounds, the ranking of the overall reaction rates under the present experimental conditions was

$$i\text{-}C_4H_{10} > n\text{-}C_4H_{10} > \text{neo-}C_5H_{12} > C_3H_8 > C_2H_6$$

From this relationship, however, it could not be concluded that the less refractory constituent accelerates the decomposition of the other component in these binary mixtures. This is because the decomposition of the less refractory component, *i*-butane, is accelerated in the *i*-butane-neopentane mixture, and a great accelerating effect is produced in the propane-neopentane mixture, despite the slight difference in reaction rates of the constituents. This suggests the necessity of taking into account the elementary reaction scheme. As shown in **Appendix 2**, the concentration of each carrier, such as hydrogen atoms, methyl radicals, and ethyl radicals, is the determining factor of the overall decomposition rates. Generally, methyl radicals are considered to have an important role in the pyrolysis of paraffinic hydrocarbons since methyl radicals are in higher concentration than other free radicals under the experimental conditions.

**Table 1 Observed overall reaction rates of $C_2H_6$, $C_3H_8$, $n$-$C_4H_{10}$, $i$-$C_4H_{10}$, and neo-$C_5H_{12}$ in single and binary systems**

| Feed | Temp. [°C] | $C_o$ [mole/$l$] | Overall reaction rate [mole/$l$·sec] single syst. ($R_p^s$) | Overall reaction rate [mole/$l$·sec] binary syst. ($R_p^b$) | $\frac{R_p^b - R_p^s}{R_p^s} \times 100$ [%] |
|---|---|---|---|---|---|
| $C_3H_8$ | 660 | 0.00218 | $7.8\times10^{-5}$ | $1.3\times10^{-4}$ | + 67 |
| $i$-$C_4H_{10}$ | | 0.00218 | $1.9\times10^{-4}$ | $2.1\times10^{-4}$ | + 11 |
| $C_3H_8$ | 660 | 0.00218 | $7.8\times10^{-5}$ | $1.0\times10^{-4}$ | + 28 |
| $i$-$C_4H_{10}$ | | 0.00109 | $6.2\times10^{-5}$ | $6.2\times10^{-5}$ | 0 |
| $C_3H_8$ | 686 | 0.00212 | $1.9\times10^{-4}$ | $3.4\times10^{-4}$ | + 79 |
| $i$-$C_4H_{10}$ | | 0.00212 | $4.0\times10^{-4}$ | $4.6\times10^{-4}$ | + 15 |
| $C_3H_8$ | 651 | 0.00220 | $6.1\times10^{-5}$ | $9.4\times10^{-5}$ | + 54 |
| $i$-$C_4H_{10}$ | | 0.00220 | $1.3\times10^{-4}$ | $1.2\times10^{-4}$ | − 8 |
| $C_3H_8$ | 660 | 0.00218 | $7.8\times10^{-5}$ | $2.2\times10^{-4}$ | +182 |
| neo-$C_5H_{12}$ | | 0.00218 | $1.1\times10^{-4}$ | $1.3\times10^{-4}$ | + 18 |
| $i$-$C_4H_{10}$ | 660 | 0.00218 | $1.9\times10^{-4}$ | $3.1\times10^{-4}$ | + 63 |
| neo-$C_5H_{12}$ | | 0.00218 | $1.1\times10^{-4}$ | $1.1\times10^{-4}$ | 0 |
| $i$-$C_4H_{10}$ | 660 | 0.00218 | $1.9\times10^{-4}$ | $1.7\times10^{-4}$ | − 11 |
| $n$-$C_4H_{10}$ | | 0.00218 | $1.4\times10^{-4}$ | $2.0\times10^{-4}$ | + 43 |
| $C_2H_6$ | 690 | 0.00633 | $2.1\times10^{-4}$ | $2.1\times10^{-4}$ | 0 |
| $C_3H_8$ | | 0.00633 | $7.9\times10^{-4}$ | $7.9\times10^{-4}$ | 0 |

From this point of view, the methyl radical concentration in the binary mixture of A and B will be mainly considered in the following discussion. For simplicity, it has been assumed that the initiation reaction is first-order and that the main termination is the methyl radical recombination. The methyl radical concentration is given, based on the steady-state approximation for the individual systems of A and B, respectively, as follows:

$$[CH_3\cdot]_A = \sqrt{\frac{k_{iA}}{k_t}C_A} \qquad (3)$$

$$[CH_3\cdot]_B = \sqrt{\frac{k_{iB}}{k_t}C_B} \qquad (4)$$

where $k_{iA}$ and $k_{iB}$ are rate constants for the initiation reactions and $k_t$ is a rate constant for the termination reaction. In the same manner as for the individual systems, the methyl radical concentration of the A–B binary system is found to be

$$[CH_3\cdot]_{A\text{-}B} = \sqrt{\frac{k_{iA}C_A + k_{iB}C_B}{k_t}} \qquad (5)$$

From Eqs. (3), (4) and (5), it is evident that the value of $[CH_3\cdot]_{A\text{-}B}$ becomes larger than that of either $[CH_3\cdot]_A$ or $[CH_3\cdot]_B$ if the values of $C_A$ and $C_B$ in

* This procedure will be acceptable when the decomposition rate equations for single and binary systems can be expressed by the same or a similar function, as pointed out by Tanji[27].

**Table 2 Reaction schemes**

| propane | *i*-butane | *n*-butane | neopentane |
|---|---|---|---|
| $C_3H_8 \xrightarrow{1} C_2H_5\cdot + CH_3\cdot$ | $i\text{-}C_4H_{10} \xrightarrow{7} CH_3\cdot + 2\text{-}C_3H_7\cdot$ | $n\text{-}C_4H_{10} \xrightarrow{12} 2\,C_2H_5\cdot$ | $\text{neo-}C_5H_{12} \xrightarrow{18} CH_3\cdot + t\text{-}C_4H_9\cdot$ |
| $C_2H_5\cdot \xrightarrow{2} H\cdot + C_2H_4$ | $2\text{-}C_3H_7\cdot \xrightarrow{6} H\cdot + C_3H_6$ | $H\cdot + n\text{-}C_4H_{10} \xrightarrow{13p} 1\text{-}C_4H_9\cdot + H_2$ | $t\text{-}C_4H_9\cdot \xrightarrow{11} H\cdot + i\text{-}C_4H_8$ |
| $H\cdot + C_3H_8 \xrightarrow{3p^*} 1\text{-}C_3H_7\cdot + H_2$ | $H\cdot + i\text{-}C_4H_{10} \xrightarrow{8p} i\text{-}C_4H_9\cdot + H_2$ | $\xrightarrow{13s} 2\text{-}C_4H_9\cdot + H_2$ | $H\cdot + \text{neo-}C_5H_{12} \xrightarrow{19} C_5H_{11}\cdot + H_2$ |
| $\xrightarrow{3s^*} 2\text{-}C_3H_7\cdot + H_2$ | $\xrightarrow{8t^*} t\text{-}C_4H_9\cdot + H_2$ | $CH_3\cdot + n\text{-}C_4H_{10} \xrightarrow{14p} 1\text{-}C_4H_9\cdot + CH_4$ | $CH_3\cdot + \text{neo-}C_5H_{12} \xrightarrow{20} C_5H_{11}\cdot + CH_4$ |
| $CH_3\cdot + C_3H_8 \xrightarrow{4p} 1\text{-}C_3H_7\cdot + CH_4$ | $CH_3\cdot + i\text{-}C_4H_{10} \xrightarrow{9p} i\text{-}C_4H_9\cdot + CH_4$ | $\xrightarrow{14s} 2\text{-}C_4H_9\cdot + CH_4$ | $C_5H_{11}\cdot \xrightarrow{21} CH_3\cdot + i\text{-}C_4H_8$ |
| $\xrightarrow{4s} 2\text{-}C_3H_7\cdot + CH_4$ | $\xrightarrow{9t} t\text{-}C_4H_9\cdot + CH_4$ | $C_2H_5\cdot + n\text{-}C_4H_{10} \xrightarrow{15p} 1\text{-}C_4H_9\cdot + C_2H_6$ | termination** |
| $1\text{-}C_3H_7\cdot \xrightarrow{5} CH_3\cdot + C_2H_4$ | $i\text{-}C_4H_9\cdot \xrightarrow{10} CH_3\cdot + C_3H_6$ | $\xrightarrow{15s} 2\text{-}C_4H_9\cdot + C_2H_6$ | ethane |
| $2\text{-}C_3H_7\cdot \xrightarrow{6} H\cdot + C_3H_6$ | $t\text{-}C_4H_9\cdot \xrightarrow{11} H\cdot + i\text{-}C_4H_8$ | $1\text{-}C_4H_9\cdot \xrightarrow{16} C_2H_5\cdot + C_2H_4$ | $C_2H_6 \xrightarrow{22} 2\,CH_3\cdot$ |
| termination** | termination** | $2\text{-}C_4H_9\cdot \xrightarrow{17} CH_3\cdot + C_3H_6$ | $H\cdot + C_2H_6 \xrightarrow{23} C_2H_5\cdot + H_2$ |
| | | $C_2H_5\cdot \xrightarrow{2} H\cdot + C_2H_4$ | $CH_3\cdot + C_2H_6 \xrightarrow{24} C_2H_5\cdot + CH_4$ |
| | | termination** | $C_2H_5\cdot \xrightarrow{2} H\cdot + C_2H_4$ |
| | | | termination** |

* p, s, and t mean primary, secondary, and tertiary position, respectively.
** All possible reactions except $2H\cdot \longrightarrow H_2$ and $H\cdot + CH_3\cdot \longrightarrow CH_4$ are included.

**Table 3 Kinetic parameters for elementary reactions**

| Reaction | log $A$ [1/sec] or [l/mole·sec] | $E$ [kcal/mole] | $k$ (660°C) |
|---|---|---|---|
| Initiation[28] | | | |
| $C_2H_6 \longrightarrow 2CH_3\cdot$ | 14.9 | 82.5 | $3.75\times10^{-5}$ |
| $C_3H_8 \longrightarrow CH_3\cdot + C_2H_5\cdot$ | 15.9 | 81.5 | $6.44\times10^{-4}$ |
| $i\text{-}C_4H_{10} \longrightarrow CH_3\cdot + 2\text{-}C_3H_7\cdot$ | 15.9 | 79.5 | $1.89\times10^{-3}$ |
| $n\text{-}C_4H_{10} \longrightarrow 2C_2H_5\cdot$ | 16.3 | 80.5 | $2.77\times10^{-3}$ |
| $\text{neo-}C_5H_{12} \longrightarrow CH_3\cdot + t\text{-}C_4H_9\cdot$ | 16.1 | 78.3 | $5.88\times10^{-3}$ |
| $RH + H\cdot \longrightarrow R\cdot + H_2$[1-3] | | | |
| $C_2H_6$ | 11.12 | 9.7 | $7.04\times10^{8}$ |
| $C_3H_8$ | 10.78 | 7.8 | $9.62\times10^{8}$ |
| $n\text{-}C_4H_{10}$ | 10.90 | 7.5 | $1.39\times10^{9}$ |
| $i\text{-}C_4H_{10}$ | 11.00 | 6.8 | $2.55\times10^{9}$ |
| $RH + CH_3\cdot \longrightarrow R\cdot + CH_4$[11] | | | |
| $C_2H_6$ | 8.49 | 10.5 | $1.07\times10^{6}$ |
| $n\text{-}C_4H_{10}$ | 8.23 | 8.5 | $1.73\times10^{6}$ |
| $i\text{-}C_4H_{10}$ | 8.37 | 8.3 | $2.67\times10^{6}$ |
| $\text{neo-}C_5H_{12}$ | 8.53 | 10.3 | $1.31\times10^{6}$ |
| Radical scission[14,15] | | | |
| $C_2H_5\cdot \longrightarrow C_2H_4 + H\cdot$ | 14.48 | 39.5 | $1.67\times10^{5}$ |
| $1\text{-}C_3H_7\cdot \longrightarrow C_2H_4 + CH_3\cdot$ | 13.90 | 32.0 | $2.56\times10^{6}$ |
| $2\text{-}C_3H_7\cdot \longrightarrow C_3H_6 + H\cdot$ | 14.11 | 38.0 | $2.80\times10^{5}$ |

Eqs. (3) and (4) are equal to those in Eq. (5). For convenience, let $C_A$ equal $C_B$, then the degree of increase of the methyl radical concentration, i.e. $[CH_3\cdot]_{A\text{-}B}/[CH_3\cdot]_A$ or $[CH_3\cdot]_{A\text{-}B}/[CH_3\cdot]_B$, depends on the initiation reaction rate constant of each component. If $k_{iA}<k_{iB}$, it is larger for the component A and is relatively small for the component B. It may, therefore, be concluded that the initiation reaction rates of the individual components are the principal determinants of the accelerating effect of the overall decomposition rates. According to the literature[28] the order of the initiating reaction rate constant at 660°C is as follows:

$$\text{neo-}C_5H_{12} > n\text{-}C_4H_{10} > i\text{-}C_4H_{10} > C_3H_8 > C_2H_6$$

This relationship indicates that the decomposition of propane is more significantly accelerated by neopentane than by *i*-butane. Indeed, this consideration receives support from the experimental results. However, the observations show that the decomposition of *n*-butane, from which initiating free radicals are generated more easily, is accelerated in the *n*-butane-*i*-butane mixture. Therefore, one cannot accurately estimate the acceleration effect based only on the information for initiation reaction rates. Actually, various termination reactions in addition to methly radical recombination participate in the overall reaction, so that the analysis of the acceleration effect becomes more complicated. Furthermore, the concentrations of hydrogen atoms and ethyl radicals also have a significant role in the overall reaction rate. More accurate values of these concentrations should be estimated according to the free-radical chain mechanism. The reaction schemes were taken from the literature[4,6,7,17,22,23,25] and are shown in **Table 2**. Rate constants used for the individual steps, except the termination steps in the schemes, were reviewed carefully from the literature[1,2,3,11,14,15,28]* and were modified for our use. The same rate constant was assigned to all of the possible termination reactions since published rate constants for various terminations were nearly equal[5]. The rate constants cited from the literature are shown in **Table 3**. First, the adequacy of the rate constants was examined by using the experimental results of the individual compounds. Based on the schemes in Table 2, the overall reaction rates were calculated by the steady-state and the long-chain approximations** (see Appendix 2), and were compared with the observed values. However, the calculated overall reaction rate of propane pyrolysis, for example, was much smaller than the experimental value at 660°C

* For H-atom abstraction reactions of alkyl radicals, it has been recently shown[16,20,21] that the Arrhenius parameters obtained at low temperatures differ from those obtained at high temperatures. However, we adopted the Arrhenius parameters obtained by low-temperature experimental data because few high-temperature data had been reported.

** Free-radical concentrations in the neopentane system were computed by the Runge-Kutta-Gill method with no approximation of the steady state and the long chain since the initiation reaction rate of neopentane is relatively high.

with a nitrogen/propane mole ratio of 5. Some modification of rate constants was required in order to fit the overall reaction rate to the results obtained. Modified rate constants as well as literature values at 660°C are given in **Table 4**. The modification of rate constants for other systems was performed systematically with reference to the modified results for the propane system. Their modified results are also given in Table 4. In every system it was necessary to increase by about 4 times the literature values of the rate constants for the H-atom abstraction reactions by a methyl radical. The scission reactions of free radicals having three or more carbon atoms were divided into two main classes: one is via the rupture of a carbon-carbon bond and the other is via the rupture of a carbon-hydrogen bond. One-fifth of the literature values for the scission reactions of 1-propyl and 2-propyl radicals were commonly given for the rate constants of the former and latter classes, respectively. The scission reaction of an ethyl radical is similar to that of a 2-propyl radical, but about one-fourth of the revised value for a 2-propyl radical was given to the value of the rate constant for an ethyl radical, since the latter is more stable than the former. The value for reaction (15) in Table 4 was estimated from the experimental values of ethane to hydrogen mole ratio in the products (see **Appendix 3**), since not as much imformation was available for the H-atom abstraction reaction by an ethyl radical as for the H-atom abstraction reactions by a hydrogen atom or a methyl radical. The overall reaction rates calculated at 660°C by using the revised rate constants versus the initial concentrations of the reactants are compared with the experimental results in **Fig. 7** (p. 288) for propane and *i*-butane.

The above reaction schemes and revised rate constants were employed to simulate the pyrolysis of binary mixtures. Three of the five individual compounds studied in this paper, propane, *i*-butane, and neopentane, have the same chain carriers of a hydrogen atom and a methyl radical, so that binary mixtures composed of these three compounds have the same chain carriers. Therefore, no new elementary reactions in addition to the combined reaction schemes for the mixtures are necessary to simulate the pyrolysis of propane-*i*-butane, propane-neopentane, and *i*-butane-neopentane mixtures. On the other hand, ethane and *n*-butane have an ethyl radical as one of the chain carriers, and thus additional new elementary reactions are perhaps required in systems which include one of these components. The new reactions expected to occur in the *n*-butane-*i*-butane and ethane-propane mixtures are shown in Eqs. (6) and (7), respectively.

$$C_2H_5\cdot + i\text{-}C_4H_{10} \xrightarrow{25} C_2H_6 + C_4H_9\cdot \qquad (6)$$

**Table 4 Rate contants[a] for elementary reactions at 660°C**

| System | Reaction No.** | Literature value | Ref. | Modified value | Note |
|---|---|---|---|---|---|
| propane | 1 | $6.44\times10^{-4}$ | (28) | * | |
| | 2 | $1.67\times10^{5}$ | (14) | $1.5\times10^{4}$ | $\frac{k_{3s}}{k_{3p}}=\frac{k_{4s}}{k_{4p}}$ |
| | 3 | $9.62\times10^{8}$ | ( 2) | * | $=1.2$[d] |
| | 4 | $1.5\times10^{6}$ | ( b) | $6.0\times10^{6}$ | |
| | 5 | $2.56\times10^{6}$ | (15) | $5.1\times10^{5}$ | |
| | 6 | $2.80\times10^{5}$ | (15) | $5.6\times10^{4}$ | |
| *i*-butane | 7 | $1.91\times10^{-3}$ | (28) | * | |
| | 8 | $2.55\times10^{9}$ | ( 3) | $(1.4\times10^{9})$ | $\frac{k_{8t}}{k_{8p}}=\frac{k_{9t}}{k_{9p}}$ |
| | 9 | $2.67\times10^{7}$ | (11) | $7.5\times10^{6}$ | $=1.25$[d] |
| | 10 | $5.1\times10^{5}$ | ( b) | * | |
| | 11 | $5.6\times10^{4}$ | ( b) | * | |
| *n*-butane | 12 | $2.77\times10^{-3}$ | (28) | * | |
| | 13 | $1.39\times10^{9}$ | ( 3) | * | $\frac{k_{13s}}{k_{13p}}=\frac{k_{14s}}{k_{14p}}$ |
| | 14 | $1.73\times10^{6}$ | (11) | $6.9\times10^{6}$ | |
| | 15 | $3.3\times10^{6}$ | ( b) | * | $=\frac{k_{15s}}{k_{15p}}=2$[d] |
| | 16 | $5.1\times10^{5}$ | ( b) | * | |
| | 17 | $5.1\times10^{5}$ | ( b) | * | |
| neopentane | 18 | $5.88\times10^{-3}$ | (28) | $3.9\times10^{-3}$ | |
| | 19 | $8.4\times10^{8}$ | ( b) | $(2.8\times10^{8})$ | |
| | 20 | $1.31\times10^{6}$ | (11) | $5.2\times10^{6}$ | |
| | 21 | $5.1\times10^{5}$ | ( b) | * | |
| ethane | 22 | $3.75\times10^{-5}$ | (28) | $1.9\times10^{-4}$ | |
| | 23 | $7.04\times10^{8}$ | ( 1) | * | |
| | 24 | $1.07\times10^{6}$ | (11) | $4.3\times10^{6}$ | |
| all syst. termination | | $1.0\times10^{11}$ | ( c) | * | |

a) [1/sec] or [*l*/mole·sec]
b) These values are estimated by authors.
c) Equal value is assumed for all possible termination reactions.
d) These values are experimentally determined by product distributions.
* Same value as literature value is used.
** Reaction numbers refer to Table 2.

$$C_2H_5\cdot + C_3H_8 \xrightarrow{26} C_2H_6 + C_3H_7\cdot \qquad (7)$$

The initial free-radical concentrations and the overall reaction rate in the propane-*i*-butane mixture, at 660°C with initial concentration, $C_o=0.00218$ mole/*l*, were calculated by combining the reaction schemes of propane and *i*-butane in Table 2 and using the revised rate constants. The results showed the acceleration of the decomposition rates of propane and *i*-butane by 30% and 16%, respectively. The agreement with the experimental results in Table 1 is good for a first estimate. Some decrease in the value of $k_8$ gave a precise fit. However, no correction of the value of $k_8$ had been suggested from the previous examination of the pyrolysis of pure *i*-butane, since its value had no effect on the overall reaction rate of pure *i*-butane. This means that the satisfactory modification of rate constants cannot be achieved from the examination of the result of pyrolysis of pure substance alone. In the same manner, a correction was required to the value of $k_{19}$, which had not previously affected the overall reaction rate of the pure neopentane pyrolysis. The corrected values used in the calculation below are shown in parentheses in the revised-value column in Table 4. Part of the

**Table 5 Calculated results of overall reaction rates and radical concentrations**

| Feed | Temp. [°C] | $C_o$ [mole/$l$] | $R_p \times 10^4$ [mole/$l$·sec] | Radical concentration [mole/$l$] H· | $CH_3$· | $C_2H_5$· |
|---|---|---|---|---|---|---|
| Single system: | | | | | | |
| $C_3H_8$ | 660 | 0.00218 | 0.89 | $2.4\times10^{-11}$ | $3.2\times10^{-9}$ | $1.1\times10^{-10}$ |
| $i$-$C_4H_{10}$ | 660 | 0.00218 | 1.86 | $3.4\times10^{-11}$ | $5.1\times10^{-9}$ | — |
| $n$-$C_4H_{10}$ | 660 | 0.00218 | 1.44 | $9.8\times10^{-12}$ | $6.3\times10^{-9}$ | $1.9\times10^{-9}$ |
| neo-$C_5H_{12}$ | 660 | 0.00218 | 1.16 | $1.4\times10^{-11}$ | $9.1\times10^{-9}$ | — |
| $C_2H_6$ | 690 | 0.00633 | 1.91 | $3.7\times10^{-11}$ | $3.0\times10^{-10}$ | $6.9\times10^{-9}$ |
| $C_3H_8$ | 690 | 0.00633 | 8.36 | $5.7\times10^{-11}$ | $1.0\times10^{-8}$ | $5.7\times10^{-10}$ |
| Binary System: | | | | | | |
| $C_3H_8$ | 660 | 0.00218 | 1.40 (+ 57)* | $3.6\times10^{-11}$ | $5.2\times10^{-9}$ | $1.1\times10^{-10}$ |
| $i$-$C_4H_{10}$ | | 0.00218 | 1.92 (+ 3) | | | |
| $C_3H_8$ | 660 | 0.00218 | 1.97 (+118) | $4.3\times10^{-11}$ | $8.4\times10^{-9}$ | $1.1\times10^{-10}$ |
| neo-$C_5H_{12}$ | | 0.00218 | 1.26 (+ 9) | | | |
| $i$-$C_4H_{10}$ | 660 | 0.00218 | 2.84 (+ 52) | $4.6\times10^{-11}$ | $9.1\times10^{-9}$ | — |
| neo-$C_5H_{12}$ | | 0.00218 | 1.35 (+ 16) | | | |
| $i$-$C_4H_{10}$ | 660 | 0.00218 | 1.99 (+ 7) | $2.4\times10^{-11}$ | $7.0\times10^{-9}$ | $2.3\times10^{-9}$ |
| $n$-$C_4H_{10}$ | | 0.00218 | 1.94 (+ 35) | | | |
| $C_2H_6$ | 690 | 0.00633 | ① 2.37 (+ 21) | $4.8\times10^{-11}$ | $5.1\times10^{-9}$ | $8.5\times10^{-9}$ |
| $C_3H_8$ | | 0.00633 | ① 7.43 (− 11) | | | |
| | | | ② 3.16 (+ 65) | $4.3\times10^{-11}$ | $2.9\times10^{-9}$ | $1.1\times10^{-8}$ |
| | | | ② 4.30 (− 51) | | | |

* The values in parentheses are the change of reaction rates: $100\times(R_p^b - R_p^s)/R_p^s$ [%]; where $R_p^s$ and $R_p^b$ mean the reaction rates in single and binary systems, respectively.

calculated results of the *i*-butane-neopentane mixture are given in **Table 5** with the results of the propane-*i*-butane and propane-neopentane mixtures. The agreement with the experimental results shown in Table 1 is good in each case. For the *i*-butane-neopentane mixture, particularly, the satisfactory agreement achieved without any modification shows that the pyrolysis of the mixtures can be simulated on the basis of the reaction schemes and the rate constants of the individual constituents. The tabulated data clearly confirm that the accelerating effect is due to the change of the concentrations of chain carriers, such as hydrogen atoms and methyl radicals. Similar calculations were performed in the propane-*i*-butane mixture at temperatures 651 and 686°C with propane/*i*-butane mole ratio=1, and further at 660°C with propane/*i*-butane mole ratio=2. These results also agreed well with the observed values.

As mentioned previously, the *n*-butane-*i*-butane and ethane-propane mixtures have ethyl radicals as one of the chain carriers and are systems in which the accelerating effect cannot be inferred even qualitatively from the information available on the initiation reaction rate of each component. In order to simulate the pyrolysis of these systems, the rate constants $k_{25}$ and $k_{26}$, of the reactions (25) and (26) given in Eqs. (6) and (7), respectively, were determined: the value of $k_{25}$ was obtained as $2.77\times10^6$ $l$/mole·sec at 660°C from the experimental value of ethane to ethylene mole ratio in the products of the *n*-butane-*i*-butane mixture (see Appendix 3), and the value of $k_{26}$ was assumed to be 10% smaller than that of $k_{15}$. The result calculated by combining the reaction (25) and the reaction schemes shown in Table 2 is given in Table 5. The calculated results agree well with the experimental observations listed in Table 1. The increase in the rate of *n*-butane decomposition can be considered to be due to the increase of the hydrogen atom concentration, while the rate of *i*-butane seems to reflect various factors such as the decrease of hydrogen atom concentration, increase of methyl radical concentration, and the effect of the addition of reaction (25). The calculated result in the ethane-propane system is also shown in Table 5. For comparison, column ② presents the result when reaction (26) was excluded and shows the great changes of the reaction rates of both components. This confirms that reaction (26) has an important role in the ethane-propane mixture.

The experimental results in all five binary mixtures could be elucidated by considering the free-radical chain reaction mechanism of the individual constituents. The procedure adopted here may be applied generally to various paraffinic hydrocarbon mixtures.

## Conclusion

The paraffinic hydrocarbons, ethane, propane, *n*-butane, *i*-butane, and neopentane, and five binary mixtures composed of these compounds were pyrolyzed at small extents of reaction by a conventional flow apparatus. From the experimental results of these mixtures, it was observed that the reaction of one component is clearly accelerated, while that of the other is hardly affected by the coexisting component. However, the degree of the acceleration varies in a

complex manner according to the specific mixture. The decomposition rate of propane increases by a maximum of 2.8 times in the propane-neopentane mixture. The product distributions from single components and mixtures are uniform with the extents of reaction, and show that the selectivity to products of a single component is maintained in its mixture system.

The experimental results in all five binary mixtures could be elucidated by combining the free-radical chain reaction schemes of the individual constituents. These schemes quantitatively show that the accelerating effect of the reaction rate is due to the change of the concentration of chain carriers, such as hydrogen atoms, methyl radicals, and ethyl radicals.

### Appendix 1

As an example, the calculation procedure for the product distributions of the propane-*i*-butane mixture is described below. The product distributions of pure propane and *i*-butane at 660°C are given by the method previously proposed

$$100\,C_3H_8 \longrightarrow 55\,H_2+45\,CH_4+45\,C_2H_4+55\,C_3H_6 \quad \text{(A-1-1)}$$

$$100\,i\text{-}C_4H_{10} \longrightarrow 56\,H_2+44\,CH_4+44\,C_3H_6+56\,i\text{-}C_4H_8 \quad \text{(A-1-2)}$$

On the other hand, the product distribution of each component in the mixture can be obtained by multiplying the conversion to both sides of the above equations. If $x_{C_3H_8}=0.056$ and $x_{i\text{-}C_4H_{10}}=0.072$ at $t=0.77$ sec, the number of moles of products per 100 moles of each component charged can be calculated as

$$5.6\,C_3H_8 \longrightarrow 3.1\,H_2+2.5\,CH_4+2.5\,C_2H_4+3.1\,C_3H_6 \quad \text{(A-1-3)}$$

$$7.2\,i\text{-}C_4H_{10} \longrightarrow 4.0\,H_2+3.2\,CH_4+3.2\,C_3H_6+4.0\,i\text{-}C_4H_8 \quad \text{(A-1-4)}$$

By adding Eqs. (A-1-3) and (A-1-4), the initial product distribution of the propane-*i*-butane mixture can be shown by

$$5.6\,C_3H_8+7.2\,i\text{-}C_4H_{10} \longrightarrow 7.1\,H_2+5.7\,CH_4+2.5\,C_2H_4+6.3\,C_3H_6+4.0\,i\text{-}C_4H_8 \quad \text{(A-1-5)}$$

Product gas composition given as mole per cent is then as follows:

$H_2$: 28, $CH_4$: 22, $C_2H_4$: 10, $C_3H_6$: 24, $i$-$C_4H_8$: 16

### Appendix 2

The overall decomposition rate of propane, for example, can be expressed in the following equation by the long-chain approximation based on the reaction scheme in Table 2.

$$-\frac{d[C_3H_8]}{dt}=k_3[H\cdot][C_3H_8]+k_4[CH_3\cdot][C_3H_8] \quad \text{(A-2-1)}$$

where $k_3=k_{3p}+k_{3s}$ and $k_4=k_{4p}+k_{4s}$

Therefore, the initial overall reaction rate is calculated by substituting free-radical concentrations and initial concentration of propane into Eq. (A-2-1).

### Appendix 3

Rates of formation of hydrogen and ethane during the initial stage of the pyrolysis of *n*-butane can be written as

$$\frac{d[C_2H_6]}{dt}=k_{15}[C_2H_5\cdot][n\text{-}C_4H_{10}] \quad \text{(A-3-1)}$$

$$\frac{d[H_2]}{dt}=k_2[C_2H_5\cdot] \quad \text{(A-3-2)}$$

From the above equations

$$\frac{d[C_2H_6]/dt}{d[H_2]/dt}=\frac{k_{15}[n\text{-}C_4H_{10}]}{k_2}\cong\frac{[C_2H_6]}{[H_2]} \quad \text{(A-3-3)}$$

Therefore, the approximate value of $k_{15}$ is obtained by substituting observed ethane/hydrogen mole ratio and initial concentration of *n*-butane into Eq. (A-3-3).

Similarly, the value of $k_{25}$ is obtained from the pyrolysis data of *n*-butane-*i*-butane mixture as follows:

$$\frac{[C_2H_6]}{[H_2]}=\frac{k_{15}[n\text{-}C_4H_{10}]+k_{25}[i\text{-}C_4H_{10}]}{k_2} \quad \text{(A-3-4)}$$


### Acknowledgment

The authors are indebted to Professor Akira Amano for valuable discussions. Thanks are also due to Mr. Mitsuo Oikawa and Mr. Akira Ushio for their assistance in the experimental work. Numerical calculation was carried out on the high-speed digital computer, NEAC 2200, of Tohoku University.


### Nomenclature

| | | | |
|---|---|---|---|
| $A$ | = | frequency factor | [1/sec] or [*l*/mole·sec] |
| $C$ | = | concentration | [mole/*l*] |
| $C_o$ | = | initial concentration | [mole/*l*] |
| $E$ | = | activation energy | [kcal/mole] |
| $F$ | = | average total flow rate of reactant gas | [cm³/sec] |
| $k_i$ | = | initiation reaction rate constant | [1/sec] |
| $k_t$ | = | termination reaction rate constant | [*l*/mole·sec] |
| $P$ | = | system pressure | [mmHg] |
| $R_p$ | = | reaction rate | [mole/*l*·sec] |
| $t$ | = | average residence time | [sec] |
| $T_{av}$ | = | effective reaction temperature | [°K] |
| $V_{av}$ | = | effective reactor volume | [cm³] |

### Literature Cited


1) Baldwin, R. R. and A. Melvin: *J. Chem. Soc.*, 1785 (1964)
2) Baldwin, R. R.: *Trans. Faraday Soc.*, **60**, 527 (1964)
3) Baldwin, R. R. and R. W. Walker: *ibid.*, **60**, 1236 (1964)
4) Baronnet, F., M. Dzierzynski, G.M. Côme, R. Martin and M. Niclause: *Inter. J. Chem. Kinetics*, **3**, 197 (1971)
5) Blakemore, J. E. and W. H. Corcoran: *Ind. Eng. Chem., Process Design and Develop.*, **8**, 206 (1969)
6) Buekens, A. G. and G. F. Froment: *ibid.*, **7**, 435 (1968)
7) Buekens, A. G. and G. F. Froment: *ibid.*, **10**, 309 (1971)
8) Davis, H. G. and K. D. Williamson: Fifth World Petroleum Congress Proc., Section 4, p. 37 (1959)
9) Gavalas, G. R.: *Chem. Eng. Sci.*, **21**, 133 (1966)
10) Haraguchi, T., F. Nakashio and W. Sakai: Preprint of the 37th Annual Meeting of The Soc. of Chem. Engrs., Japan, E-103, Nagoya (1972)
11) Kerr, J. A. and A. F. Trotman-Dickenson: *J. Chem. Phys.*, **19**, 163 (1951)
12) Kershenbaum, L. S. and J. J. Martin: *AIChE J.*, **13**, 148 (1967)
13) Kubota, K. and N. Morita: *J. Chem. Soc., Japan*, **72**, 616 (1969)
14) Laidler, K. J. and B. W. Wojciechowski: Proc. Roy. Soc. (London), A260, 91 (1961)
15) Laidler, K. J., N. H. Sagert and B. W. Wojciechowski: *ibid.*, A270, 242 (1962)
16) Leathard, D. A. and J. H. Purnell: *Ann. Rev. of Phys. Chem.*, **21**, 197 (1970)
17) Lin, M. C. and M. H. Back: *Can. J. Chem.*, **44**, 505 (1966)
18) Murata, M., S. Saito, A. Amano and S. Maeda: *J. Chem. Eng. Japan*, **6**, 252 (1973)
19) Murata, M., N. Takeda, S. Saito, A. Amano and S. Maeda: Preprint of the 6th Autumn Meeting of The Soc. of Chem. Engrs., Japan, C-208, Tokyo (1972)
20) Pacey, P. D. and J. H. Purnell: *Inter. J. Chem. Kinetics*, **4**, 657 (1972)

21) Pacey, P. D. and J. H. Purnell: *J. Chem. Soc. Trans. Faraday*, Div. I, **68**, 1462 (1972)
22) Purnell, J. H. and C. P. Quinn: Proc. Roy. Soc. (London), A270, 267 (1962)
23) Quinn, C. P.: *ibid.*, A275, 190 (1963)
24) Robinson, K. K. and E. Weger: *Ind. Eng. Chem. Fundamentals*, **10**, 198 (1971)
25) Sagert, N. H. and K. J. Laidler: *Can. J. Chem. Eng.*, **41**, 838 (1963)
26) Shirotsuka, T., M. Chao, and S. Horie: Preprint of the 36th Annual Meeting of The Soc. of Chem. Engrs., Japan, D-101, Tokyo (1971)
27) Tanji, H.: Ph.D. thesis of Tohoku University (1968)
28) Tsang, W.: *Inter. J. Chem. Kinetics*, **1**, 245 (1969)
29) Towell, G. D. and J. J. Martin: *AIChE J.*, **7**, 693 (1961)
30) Zdonik, S. B., E. J. Green, and L. P. Hallee: *The Oil and Gas Journal*, 192 (July 10, 1967)
31) Zdonik, S. B., E. J. Green and L. P. Hallee: *ibid.*, 112 (October 16, 1967)

# THE BEHAVIOR OF AGGLOMERATES UNDER TENSILE STRAIN*

H. RUMPF AND H. SCHUBERT
*Institut für Mechanische Verfahrenstechnik der Universität Karlsruhe, Germany*

**This paper deals with the tensile strength and strain behavior of agglomerates. For moist agglomerates the tensile strength in the whole region of liquid saturation may be described. The theory agrees well with the experimental results. For agglomerates bound together by liquid bridges, a model which reproduces the force-displacement behavior of agglomerates under unidirectional loading is proposed. The validity of this model is demonstrated with the help of a specially developed apparatus which enables the strain for a given force to be measured. The theoretically and experimentally determined stable and unstable regions of the stress-strain curves of the agglomerates are discussed.**

## 1. Introduction

Strength is one of the most important attributes of an agglomerate. We regard strength as including all properties expressing the resistance of the agglomerate to possible external forces acting upon it. Since there are many different number of ways in which external forces can act on an agglomerate, strength is not a tightly defined concept. Attempts are therefore made to simulate, by suitable test methods, the forces which actually occur. From these methods, which measure for instance the resistance to impact, bending, cutting, dropping or abrasion, certain strength characteristics can be derived. They are, however, unsuitable for theoretical descriptions because in general we do not know the stresses which provoke a fracture.

There are two important strength parameters for the occurrence of a fracture within the material under stress, viz. the tensile strength and the shear strength. If the maximum principal tensile stress exceeds the tensile strength at any point of the material, a brittle fracture forms. If the shear stress at any cross-section is greater than the shear strength, shearing will occur at this cross-section. The tensile and shear strength thus provide approximate characteristics for the strength behaviour of the material.

As we shall see later, the tensile strength of an agglomerate can in many cases be calculated or at least estimated. We therefore concentrated our initial studies on the determination of the tensile strength. Since agglomerates often behave like brittle substances, the tensile strength is in many cases suitable as a comparative strength value. Simultaneously we started to examine the shear behavior of moulded powder compacts[1,2].

The cohesion of an agglomerate may be due to several bonding mechanisms[3]. **Table 1** gives a summary of the most important ones. From the multitude of possible cases we shall here only single out adhesion through mobile, liquid surfaces and through van der Waals' forces. It is possible for different bonding mechanisms to be superimposed. The strain behavior of the agglomerate must also often

* Received on February 5, 1974
H. Rumpf
Institut für Mechanische Verfahrenstechnik der Universität Karlsruhe, 75 Karlsruhe, Richard-Willstätter-Allee, Germany